



Synthesis and Optical Studies on Concentration Dependent Dy³⁺ Doped Lithium Fluoroborate Glasses for W-LED Applications

V. Anthony Raj^{1,2}, I. Arul Rayappan^{2,*}

¹Department of Physics, Bishop Heber College, Trichy-620017.

²Department of Physics, St. Joseph's College, Trichy-620002.

Corresponding authors: * arulroy@gmail.com

Abstract

A new series of Dy³⁺ doped Lithium fluoroborate glasses with the chemical composition (40-x)B₂O₃ + 20ZnO + 20NaF + 20Li₂O + xDy₂O₃ (where x = 0.1, 0.3, 1.0, 2.0 and 3.0 wt%) were prepared following conventional melt quenching technique and characterized using XRD, FTIR, optical absorption and luminescence measurements. The XRD pattern of the prepared glasses confirms the amorphous in nature. The fundamental stretching vibrations of various borates (BO₃, BO₄) were identified through the FTIR analysis. From the UV-Vis-NIR spectra, the oscillator strength and bonding parameter were calculated. The ionic bond nature of the prepared glasses were identify from their negative sign of δ . The luminescence spectra exhibit two visible bands ⁴F_{9/2}→⁶H_{15/2} (Blue) and ⁴F_{9/2}→⁶H_{13/2} (Yellow) respectively. The radiative properties such as peak wavelength and effective band width for the ⁴F_{9/2}→⁶H_{15/2} and ⁴F_{9/2}→⁶H_{13/2} emission transition were calculated. The decay lifetime of the ⁴F_{9/2} level has been measured from the decay profiles and compared with the calculated lifetimes. The yellow to blue (Y/B) ratios and color coordinates have been calculated from the luminescence spectra and the utility of the present glasses for white light emitting diodes (W-LEDs) applications.

Keywords: Borate glasses, Melt quenching technique, Bonding parameter, Oscillator strengths, Life time, W-LED.

Introduction

Among the trivalent rare-earth ions, Dy³⁺ (4f⁹) is quite interesting, because Dy³⁺ doped glasses have been considered as promising luminescent materials and also most suitable to analyze the spectroscopic properties with the change in concentration as well as glass composition. Several researchers reported the luminescence properties of Dy³⁺ ions in different glass matrices [1]. For efficient luminescence from the RE ion, the selection of glass host is an important issue. Among the oxide glasses, borate glasses have been the subject of interest for quite some time due to their high transparency, low melting point, high thermal stability and good rare earth ion solubility [2]. Because borate has been chosen as a host matrix for the present work. There has been a considerable interest in the study of borate based glasses over the past few years due to their interesting structural and optical properties. A striking characteristic feature of the borate glasses is the variations in its structural properties when alkaline or alkali earth cations are introduced [3, 4]. The addition of heavy metal oxides into glasses increases the mechanical strength and radiative transition rate of the RE ions and also reduces the glass transition [5, 6]. The higher phonon energy of the borate glasses can be reduced by adding NaF which enhances the quantum efficiency and the fluoride content reduces the non-radiative decay and in turn enhances the luminescence yield [7].

Dysprosium is the best choice for white light applications because of its two dominant emission bands such as ⁴F_{9/2} →⁶H_{15/2} and ⁴F_{9/2}→⁶H_{13/2} energy levels transitions in the visible region [7-10]. The

${}^4F_{9/2} \rightarrow {}^6H_{15/2}$ emission band is due to the magnetic dipole transition and the ${}^4F_{9/2} \rightarrow {}^6H_{13/2}$ emission band is due to the electric dipole transition and this transition is highly affected by the host matrix and the intensity of the yellow emission band can be modified by the ligand field around the RE-ion site. White light can be stimulated from the Dy^{3+} doped glass materials by adjusting the yellow to blue (Y/B) intensity ratio by varying the glass composition, RE ion concentration and excitation wavelengths [11]. In the CIE 1931 chromaticity diagram, the line related between blue and yellow region usually passes through the white light region and therefore the ability of the white light emission by the Dy^{3+} doped glasses can be confirmed through the CIE color chromaticity coordinates. The better white light can be stimulated from the Dy^{3+} doped glass materials at suitable Y/B intensity ratio by selecting the different ligand field strengths.

The aim of the present work is (i) to prepare Dy^{3+} doped lithium fluoroborate glasses following the melt quenching technique with varying Dy^{3+} ion concentrations; (ii) to identify the different vibrational bands of the borate network in the prepared glasses; (iii) to evaluate the predominant covalent/ionic nature and to determine the direct and indirect band gaps from the absorption spectra; (iv) to calculate the oscillator strengths and Judd-Ofelt parameters (Ω_2 , Ω_4 , Ω_6) from the absorption energy levels and refractive index of the prepared glasses; (v) to study the luminescence characteristics of the thermally coupled energy level transition ${}^6F_{11/2} \rightarrow {}^6H_{15/2}$ in the visible region and the ${}^6H_{11/2} \rightarrow {}^6H_{15/2}$ transition in the NIR region; (vi) to calculate the radiative parameters of the desired transitions; (vii) to determine the stimulated emission cross-section of the ${}^4F_{9/2} \rightarrow {}^6H_{15/2}$ and ${}^4F_{9/2} \rightarrow {}^6H_{13/2}$ transitions (viii) to determine the optical gain bandwidth and figure of merit of the ${}^4I_{13/2} \rightarrow {}^6H_{15/2}$ transition. (ix) The characteristic of the emission color was examined through CIE 1931 chromaticity diagram. And finally (x) Decay curves of the ${}^4F_{9/2}$ energy level have been measured and the possibility of energy transfer

between Dy^{3+} - Dy^{3+} ions in the prepared glasses have also been discussed and reported.

Experimental

The Dy^{3+} doped lithium fluoroborate glasses were prepared with the composition $(40-x)B_2O_3 + 20ZnO + 20NaF + 20Li_2O + xDy_2O_3$ (where $x = 0.1, 0.3, 1.0, 2.0$ and 3.0 wt%) using conventional melt quenching technique. The Glass Samples are labeled as BZL0.1D, BZL0.3D, BZL1.0D, BZL2.0D and BZL3.0D respectively. All the precursors used for the preparation of glasses are of high purity analytical grade (99.99%) from Sigma Aldrich. About 12g batch of the chemicals were weighted and ground thoroughly in an agate mortar to obtain a homogeneous mixture. The mixture was taken in a porcelain crucible and heated to $950^\circ C$ in an electrical furnace for 2 hour. The melt was then poured on to a preheated brass plate and kept at $350^\circ C$ for 7 h in order to remove strains from the annealing process. The glasses were slowly cooled to room temperature (RT). The prepared glasses were well polished on both sides to obtain optical quality glasses for optical measurements.

The XRD patterns were recorded by using JEOL 8030 X-ray diffractometer employing $CuK\alpha$ radiation. The infrared transmittance spectra of the prepared glasses were recorded using JASCO FTIR 460 plus in the mid-IR region ($400-4000\text{ cm}^{-1}$) with a spectral resolution of $\pm 1.0\text{ cm}^{-1}$ and 16 scans per sample. The absorption spectral measurements were made employing Perkin-Elmer Lambda 950 UV-vis-NIR spectrophotometer in the wavelength range 350–1800 nm. The luminescence spectra were recorded in the wavelength range 500–600 nm with JobinYvon Fluorolog-3 spectrofluorometer using xenon lamp (450 W) as an excitation source. Luminescence spectra in the wavelength region 1400–1700 nm were recorded using EG&G Princeton Applied Research model 5210 with a spectral resolution of $\pm 0.5\text{ nm}$. The decay measurements were made employing the FLS 920 Edinburgh spectrometer. All the measurements were carried out as room

temperature (RT) only. The physical properties of prepared glasses were calculated using the relevant expressions reported in literature [12] and the results are presented in Table 1.

Results and discussion

XRD Analysis

The X-ray diffraction (XRD) pattern has been recorded in the range $10^\circ \leq \theta \leq 80^\circ$. The XRD pattern of the BZL1.0D glass shown in figure 1. The XRD Pattern does not exhibit any detectable sharp characteristics peak, but the broad diffused scattering occurs at the lower angles, which is the characteristic long range structural disorder confirms the amorphous nature and non-crystalline structure of the prepared glass. Remaining the glass samples also exhibit similar in nature, so they are not shown for the glasses in figure 1.

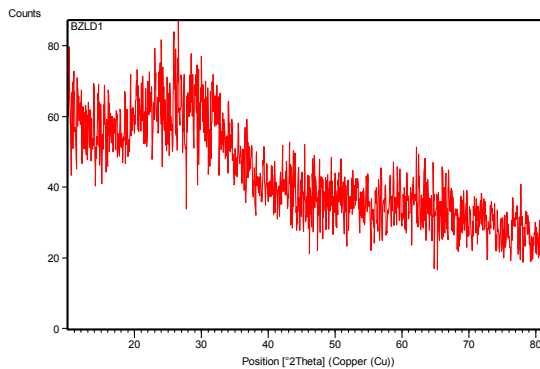


Figure 1. XRD pattern of Dy³⁺ doped lithium fluoroborate BZL1D glass

Table 1. Physical properties of the Dy³⁺ doped lithium fluoroborate glasses

Physical Properties	BZL0.1D	BZL0.3D	BZL1.0D	BZL2.0D	BZL3.0D
Density, ρ (g/cm ³)	3.064	3.233	4.620	3.537	3.626
Refractive index, n_d (589.3 nm)	1.582	1.585	1.589	1.592	1.597
Dy ³⁺ ion concentration, N_E (10 ²⁰ ions/cm ³)	0.662	2.104	9.647	14.01	20.50
Polaron radius, r_p (Å)	9966	677.3	407.7	360.0	317.1
Inter ionic distance, r_i (Å)	2472	1681	1012	893.5	787.0
Field strength, F (10 ¹⁴ cm ⁻²)	0.491	1.061	2.928	3.757	4.842
Molar refractivity, R_m (cm ³)	13.35	12.65	9.256	11.63	11.40
Dielectric constant, (ϵ)	2.502	2.512	2.524	2.534	2.550
Reflection losses, R (%)	5.080	5.121	5.175	5.216	5.284
Molar volume, V_m (cm ³ /mol)	0.109	0.349	1.601	2.327	3.405
Electronic polarizability, α_e (10 ⁻²² cm ³)	12.04	3.803	0.834	0.576	0.396

FTIR spectral studies

Figure 2 shows the FTIR spectra of the prepared glasses recorded between 400-4000 cm⁻¹. The FTIR spectra of Dy³⁺ doped lithium fluoroborate glasses and band positions corresponding to their band assignments of all the glasses matrices are given in table 2. The FTIR spectra are the powerful tool to analyze the structure of B-O network and also influenced by the addition of dopant ions. The broad absorption band around 3440-3446 cm⁻¹ is observed in all the glasses are attributed to the fundamental O-H stretching vibrations which reveals the presence of strong hydroxyl groups. The observed bands around 2620-2920 cm⁻¹ are mainly due to the occurrence of Hydrogen bonding.

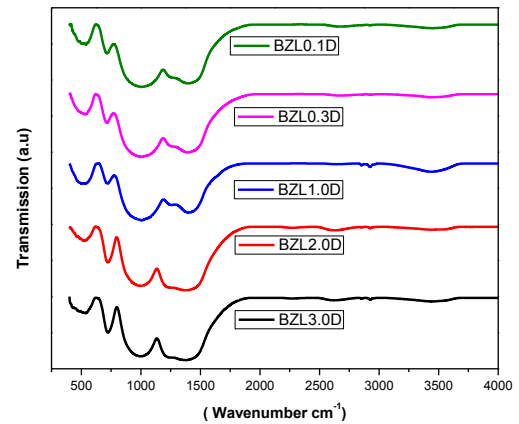


Figure 2. FTIR spectra of Dy³⁺ doped lithium fluoroborate glasses

The absorption bands centred at around 1370 cm⁻¹-1391 cm⁻¹ are attributed to B-O vibrations bond in isolated pyroborate group, trigonal boron groups and B-O bond asymmetric vibrations from pyro- and ortho-borate groups respectively. The absorption band is 991-1004 cm⁻¹, are attributed to presence of Stretching of BO₄ groups and the absence of the absorption band around 806 cm⁻¹ indicates that, there is no boroxyl ring formation in the prepared glasses. The peak at 715-720 cm⁻¹ is due to the bending vibrations of bridging oxygen in B-O-B from pentaborate groups. The asymmetric bending vibration of [BO₃] pyramidal units are

observed around 522-535 cm^{-1} . The Zn-O stretching vibrations was confirmed from the band around 450-466 cm^{-1} .

Absorption spectra

The UV-Vis-NIR absorption spectra of the Dy^{3+} doped lithium fluoroborate glasses recorded in the wavelength region between 350 nm and 2000 nm is shown in figure 3. The absorption band positions of the prepared glasses are presented in Table 3. The absorption spectra for all the prepared glasses are alike with small variations in intensities of the observed transitions and closely resemble the spectra reported for Dy^{3+} doped glasses [13]. The absorption spectra of the title glasses exhibit nine distinct in-homogeneously broadened absorption bands were observed. These absorption bands are due to the transitions from the ${}^6\text{H}_{15/2}$ ground state to the several excited states such as ${}^6\text{H}_{11/2}$, ${}^6\text{F}_{11/2}$, ${}^6\text{F}_{9/2}$, ${}^6\text{F}_{7/2}$, ${}^6\text{F}_{5/2}$, ${}^6\text{F}_{3/2}$, ${}^6\text{F}(3)_{9/2}$, ${}^4\text{I}(3)_{15/2}$ and ${}^4\text{H}(4)_{11/2}$ corresponding to the wavelengths at 1665, 1260, 1080, 890, 799, 748, 523, 447 and 421 nm respectively.

Table 2. FTIR spectra of Dy^{3+} Doped lithium fluoroborate glasses

S. No.	BZL0.1D	BZL0.3D	BZL1.0D	BZL2.0D	BZL3.0D	Assignments
1	3440	3446	3431	3440	3440	Fundamental stretching of OH group
2.	2672	2670	2920	2637	2628	Hydrogen bonding
4.	1392	1398	1398	1378	1370	B-O Stretching vibration in BO_3 units of meta, pyroborate and orthoborate groups.
5.	1004	1003	1002	997	991	Stretching of BO_4 groups
6.	717	715	717	720	716	Bending vibrations of bridging oxygen in B-O-B from pentaborate groups
7	523	535	525	529	522	Stretching vibrations of $[\text{BO}_3]$ pyramidal units
8	450	466	463	457	465	Zn-O stretching vibration

The spin allowed ($\Delta S=0$) transitions ${}^6\text{H}_{15/2} \rightarrow {}^6\text{F}_{11/2}$ possess higher absorption intensity than the other transitions and the same is observed in the lower energy region. Nephelauxetic ratios (β) were calculated from the absorption spectra using the relation $\beta = \nu_c/\nu_a$, where β is the ratio between the wavenumber (in cm^{-1}) of a particular transition of the RE ion under investigation and the wavenumber (in cm^{-1}) for the corresponding transition of an aquo-ion. Bonding parameter (δ) have been calculated from the average values of β (referred as $\bar{\beta}$) using the following expression, $\delta = (1 - \bar{\beta})/\bar{\beta}$. The nature of the bonding will be covalent or ionic depending upon the positive or negative sign of δ and the values are found to be -1.6487, -1.5779, -1.4897, -1.1083 and -1.1267 corresponding to the prepared BZL0.1D, BZL0.3D, BZL1.0D, BZL2.0D and BZL3.0D glasses respectively.

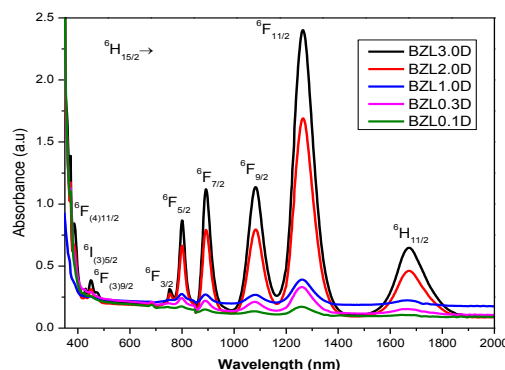


Figure 3. Absorption spectra of Dy^{3+} doped lithium fluoroborate glasses

It is observed from these results that, the bonding between Dy^{3+} ion and ligands is of ionic in nature and the ionic nature gradually decreases with the increase in Dy^{3+} ion concentration.

Oscillator strengths and Judd-Ofelt parameters

The intensity of the absorption bands can be characterized through the oscillator strength values of the f-f electronic transitions in the RE ions. The experimental oscillator strengths (f_{exp}) of the absorption bands are calculated from the relative areas under the absorption bands of the individual transition in the absorption spectra of the RE ions

doped materials. The experimental (f_{exp}), calculated (f_{cal}) oscillator strengths and rms deviation for the observed band positions of the Dy^{3+} doped lithium fluoroborate glasses are presented in table 4. Judd-Ofelt intensity parameters Ω_2 , Ω_4 , and Ω_6 , are obtained from the experimental spectral intensities and the doubly reduced matrix elements using JO theory [14]. The JO parameters have been calculated and the same are presented in table 5. The JO analysis for the Dy^{3+} ions is in good agreement with f_{exp} and f_{cal} for the intense transitions and moderate agreement in the case of weak transitions.

The JO intensity parameters of all the prepared glasses follow the trends $\Omega_2 > \Omega_4 > \Omega_6$ and is similar to the reported glasses [15-20]. The Ω_2 values are found to be higher than the Ω_4 and Ω_6 intensity parameter. The higher magnitude of Ω_2 in the present glasses suggests that degrees of covalency of Dy-O bond and higher asymmetry around the Dy^{3+} ions. The spectroscopic quality factor (Ω_4/Ω_6) is an important parameter used to describe the optical quality of the prepared glasses and is calculated from the Ω_4/Ω_6 ratio values of the prepared glasses and the results are presented in table 5. It is observed from these results that among the prepared glasses, BZL0.3D glass is 1.7460 appears to be a better optical glasses. The larger spectroscopic quality factor predicts higher stimulated emission cross section among the prepared glasses.

Table 3. Observed band positions (cm^{-1}) and bonding parameters (β and δ) Dy^{3+} doped lithium fluoroborate glasses

Transition	ENERGY					Aqua Ion (ν_0) (β)
	BZL0.1D	BZL0.3D	BZL1.0D	BZL2.0D	BZL3.0D	
${}^6H_{11/2}$	5998	6006	6006	5981	5988	5850
${}^6F_{11/2}$	7936	7924	7918	7905	7911	7700
${}^6F_{9/2}$	9285	9242	9225	9234	9233	9100
${}^6F_{7/2}$	11261	11211	11186	11211	11211	11000
${}^6F_{5/2}$	12531	12516	12500	12500	12500	12400
${}^6F_{3/2}$	13459	13333	13333	13333	13298	13250
${}^6F(3)_{9/2}$	21186	21277	21231	21142	21141	21100
${}^4I(3)_{15/2}$	22371	22371	22321	22222	22222	22100
${}^4H(4)_{11/2}$	23585	23810	23866	23310	23364	23400
β	1.0167	1.0160	1.0151	1.0112	1.0113	-
δ	-1.6487	-1.5779	-1.4897	-1.1083	-1.1267	-

Table 4. The experimental (f_{exp}) and calculated (f_{cal}) oscillator strengths (10^{-6}), number of transitions (N) and rms deviation (δ) of the Dy^{3+} doped lithium fluoroborate glasses

Transition from ${}^6H_{15/2}$	BZL0.1D		BZL0.3D		BZL1.0D		BZL2.0D		BZL3.0D	
	f_{exp}	f_{cal}								
${}^6H_{11/2}$	0.010	0.025	0.345	0.519	0.791	0.956	0.962	0.933	1.002	0.976
${}^6F_{11/2}$	0.190	0.188	3.508	3.484	5.136	5.115	4.947	4.950	4.763	4.766
${}^6F_{9/2}$	0.040	0.049	1.230	1.270	1.835	1.890	2.090	2.036	1.861	1.812
${}^6F_{7/2}$	0.700	0.035	0.941	0.852	1.279	1.804	1.336	1.591	1.353	1.593
${}^6F_{5/2}$	0.010	0.014	0.926	0.344	0.535	1.076	1.028	0.711	1.058	0.758
${}^6F_{3/2}$	0.010	0.003	0.090	0.064	0.100	0.202	0.220	0.1342	0.279	0.142
${}^6F(3)_{9/2}$	0.030	0.003	0.230	0.064	0.100	0.258	0.066	0.1205	0.117	0.121
${}^4I(3)_{15/2}$	0.030	0.008	0.260	0.171	0.278	0.153	0.332	0.0141	0.318	0.337
${}^4H(4)_{11/2}$	0.040	0.002	0.182	0.051	0.078	0.230	0.041	0.0244	0.178	0.046
N	9		9		9		9		9	
rms	0.022		0.223		0.218		0.141		0.144	

Luminescence Spectra

The Luminescence behavior of the Dy^{3+} doped Alkali lithium fluoroborate glasses have been studied through the excitation and emission spectral measurements. The excitation spectrum of the title glasses recorded by monitoring an emission at 574 nm is shown in figure 4. It exhibits six bands owing to the electronic transitions at 346nm (${}^6P_{7/2}$), 358nm (${}^4P_{3/2}$), 382nm (${}^4I_{13/2}$), 420nm (${}^4G_{11/2}$), 447nm (${}^4I_{15/2}$) and 470nm (${}^4F_{9/2}$) the transitions respectively [21, 22]. These excitation wavelength are in good agreement with the wavelength of the commercially available UV LEDs having emission range from 350 to 420 nm and blue LEDs having emission ranges from 450-470nm. The intensity of the excitation band observed at 382nm to the ${}^6H_{15/2} \rightarrow {}^4I_{13/2}$ transition is found to be higher when compared to other transitions, these transitions ${}^4I_{13/2}$ is more intense which is used to record emission spectra with excitation wavelength of 382nm. The luminescence spectra of Dy^{3+} doped Alkali lithium fluoroborate glasses were recorded by excitation 382nm are shown in figure 5. The luminescence spectra of the prepared glasses exhibit two intense emission bands in the blue (478 nm) and yellow (574 nm) region of the visible spectrum corresponding to the ${}^4F_{9/2} \rightarrow {}^6H_{15/2}$ and ${}^4F_{9/2} \rightarrow {}^6H_{13/2}$ transitions respectively. The white light can be generated in Dy^{3+} doped glass materials by UV excitation with the suitable combination of these blue and yellow emission bands.

The intensity of electric dipole transition ${}^4F_{9/2} \rightarrow {}^6H_{13/2}$ is found to be higher than the magnetic dipole transition ${}^4F_{9/2} \rightarrow {}^6H_{15/2}$. The dominant electric dipole transition is a hypersensitive in nature strongly depends upon only by the host matrix strength around the rare earth ion. The bands of the emission peaks are similar in all the glass matrices except the variations in the intensity of the emission transition.

The radiative properties such as radiative transition probability (A) effective band width ($\Delta\lambda_{\text{eff}}$) stimulated emission cross-section (σ_p^E) and branching ratios (β_R) for the ${}^4F_{9/2} \rightarrow {}^6H_{15/2}$ and ${}^4F_{9/2} \rightarrow {}^6H_{13/2}$ levels for the prepared glasses have been calculated and presented in table 6. The variations in calculated and experimental branching ratio values are probably due to the involvement of non-radiative processes. In the present work, branching ratio (β_R), and stimulated emission cross-section (σ_p^E) for the ${}^4F_{9/2} \rightarrow {}^6H_{13/2}$ lasing transition is found to be higher compared to other transitions. The higher stimulated emission cross-section value indicates the suitability of the prepared BZL1.0D glass for low threshold and high gain laser applications. The gain bandwidth and the optical gain are the two important parameters which should be considering by laser designer to fabricate new efficient visible lasers.

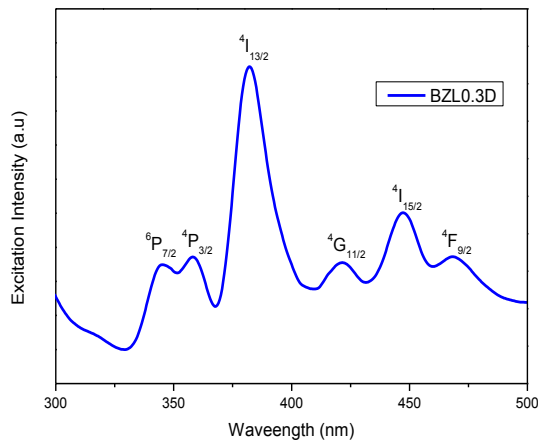


Figure 4. Excitation spectra of Dy^{3+} doped lithium fluoroborate glasses

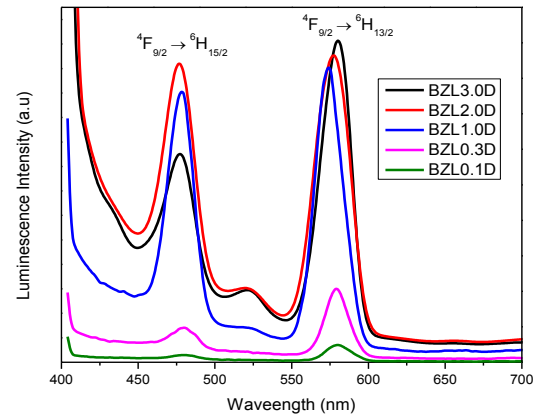


Figure 5. Luminescence spectra of Dy^{3+} doped lithium fluoroborate glasses

Table 5. Judd-Ofelt intensity parameters (Ω_λ , 10^{-20} cm^2) for the Dy^{3+} doped lithium fluoroborate glasses and other reported Dy^{3+} doped glasses

Glass code	Ω_2	Ω_4	Ω_6	Ω_4/Ω_6	Trend	Ref.
BZL0.1D	0.21	0.05	0.03	1.518	$\Omega_2 > \Omega_4 > \Omega_6$	[Present]
BZL0.3D	3.39	1.44	0.82	1.746	$\Omega_2 > \Omega_4 > \Omega_6$	[Present]
BZL1.0D	5.12	1.99	1.28	1.559	$\Omega_2 > \Omega_4 > \Omega_6$	[Present]
BZL2.0D	4.88	1.82	1.69	1.073	$\Omega_2 > \Omega_4 > \Omega_6$	[Present]
BZL3.0D	5.08	1.80	1.24	1.453	$\Omega_2 > \Omega_4 > \Omega_6$	[Present]
Lithium borate	3.24	0.92	0.82	1.122	$\Omega_2 > \Omega_4 > \Omega_6$	15
L4BA	9.85	4.35	2.47	1.761	$\Omega_2 > \Omega_4 > \Omega_6$	16
Dy:LiLTB	8.75	2.62	2.07	1.266	$\Omega_2 > \Omega_4 > \Omega_6$	17
L ₂ BTAFDy	9.36	2.87	2.82	1.018	$\Omega_2 > \Omega_4 > \Omega_6$	18
1.0LBTPD	10.30	3.53	2.79	1.265	$\Omega_2 > \Omega_4 > \Omega_6$	19
BTLN2D	6.00	1.86	1.25	1.490	$\Omega_2 > \Omega_4 > \Omega_6$	20

Table 6. Emission band position (λ_p , nm), effective band width ($\Delta\lambda_{\text{eff}}$, nm), radiative transition probability (A , s^{-1}), stimulated emission cross-section ($\sigma_p^E \times 10^{-22} \text{ cm}^2$), calculated and experimental radiative branching ratios (β_R), for the Dy^{3+} doped lithium fluoroborate glasses

Glass code	Transition s	λ_p	$\Delta\lambda_{\text{eff}}$	A	σ_p^E	β_R (cal)	β_R (exp)
BZL0.1D	${}^6H_{15/2}$	480	1.3370	3.14	0.6417	0.1447	0.0295
	${}^6H_{13/2}$	579	4.2361	18.37	2.5840	0.8735	0.1727
BZL0.3D	${}^6H_{15/2}$	480	4.1039	78.72	5.3783	0.2120	0.1361
	${}^6H_{13/2}$	579	3.6647	340.15	55.0989	0.7879	0.5882
BZL1.0D	${}^6H_{15/2}$	478	6.2528	119.83	5.2578	0.3916	0.1436
	${}^6H_{13/2}$	577	5.1518	516.20	57.7114	0.6083	0.6184
BZL2.0D	${}^6H_{15/2}$	476	5.7884	150.10	6.9697	0.3564	0.1705
	${}^6H_{13/2}$	577	6.0657	531.48	50.8483	0.6435	0.6036
BZL3.0D	${}^6H_{15/2}$	477	6.2286	116.64	5.0441	0.2751	0.1407
	${}^6H_{13/2}$	580	5.4634	514.14	55.4080	0.7249	0.6203

Energy level diagram

The figure 6 shows the partial energy level diagram of the Dy³⁺ doped lithium fluoroborate glasses along with the probable radiative and non-radiative emission transitions are presented. While exciting the Dy³⁺ doped lithium fluoroborate glasses at 384 nm the ⁴I_{13/2} excited state is more popular. Meanwhile it non-radiatively decays from the ⁴I_{13/2} to ⁴F_{9/2} lower excited state. The visible emission lines arises from the ⁴F_{9/2} excited state due to the large energy gap between the ⁴F_{9/2} energy level to the next lower level ⁶F_{3/2}. From the excited state ⁴F_{9/2} two characteristic emission transitions ⁴F_{9/2} → ⁶H_{15/2} (blue) and ⁴F_{9/2} → ⁶H_{13/2} (yellow) are observed. In addition to these, at higher concentrations cross-relaxation between adjacent Dy³⁺ ions occur, leading to the observed concentration quenching in the luminescence of the prepared glasses. The Luminescence quenching occurs by the resonant energy transfer (RET) from the ⁴F_{9/2} excited state to the nearby Dy³⁺ ions in the ground state. Generally cross-relaxation occurs only when the energy of the emission transitions perfectly match with the absorption transition. In energy cross-relaxation channels two Dy³⁺ ions, one ion in ground state and another one in the excited state interchange their energies and reach some intermediate states and then relax non-radiatively. The resonant cross relaxation channels of the Dy³⁺ doped lithium fluoroborate glasses are (⁴F_{9/2} → ⁶F_{7/2}, ⁶H_{15/2} → ⁶F_{9/2}+⁶F_{7/2}), (⁴F_{9/2} → ⁶F_{3/2}, ⁶H_{15/2} → ⁶F_{11/2}+⁶F_{9/2}) and these relaxations quenching visible emissions ⁴F_{9/2} → ⁶H_{15/2} and ⁴F_{9/2} → ⁶H_{13/2}. The Dy³⁺ ions after reaching the ⁶F_{3/2} and ⁶F_{7/2} intermediate states de-excite to the ⁶H_{15/2} ground state non-radiatively [9, 11, 23].

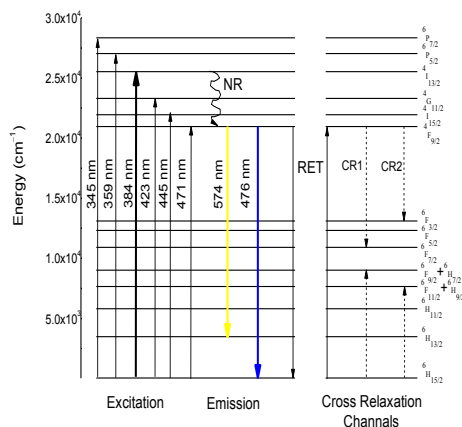


Figure 6. Energy level diagram of the Dy³⁺ doped lithium fluoroborate glasses

Decay analysis

The decay profile corresponding to the ⁴F_{9/2} excited level of the Dy³⁺ doped lithium fluoroborate glasses were measured by monitoring luminescence at 574nm under 382nm excitation as shown in fig 7. The decay curves exhibit single exponential behavior for the lower concentration glasses up to 0.3 mol % and turn into the non-exponential nature for higher concentration (≥1.0 mol % Dy³⁺). The non-exponential nature of the luminescence decays increases with increasing concentration of the Dy³⁺ ions indicating that the enhancement of energy transfer processes between the Dy³⁺ ions with increasing concentration in these matrices. The experimental life time of the prepared glasses have been obtained by using non-exponential fitting methods and can be expressed as

$$I = y_0 + A_1 \exp\left(-\frac{t}{\tau_1}\right) + A_2 \exp\left(-\frac{t}{\tau_2}\right)$$

where A₁ and A₂ are constants, τ₁ and τ₂ are the luminescence life times for the two channels responsible for the decay and the experimental lifetime (τ_{exp}) has been calculated by using the relation,

$$\tau_{\text{exp}} = \frac{A_1 \tau_1^2 + A_2 \tau_2^2}{A_1 \tau_1 + A_2 \tau_2}$$

The rate of energy transfer by cross relaxation can be represented as

$$W_{\text{NR}} = \frac{1}{\tau_{\text{exp}} - 1} \frac{1}{\tau_{\text{cal}}}$$

The quantum efficiency (η) can be defined as the ratio of number of photons emitted to the number of photons absorbed. For rare earth ions, it is the ratio between the experimental and the radiative lifetimes of the excited state can be expressed as

$$\eta = \frac{\tau_{\text{exp}}}{\tau_{\text{cal}}} \times 100$$

Table 7 represented the experimental and calculated life times (λ_{exp} and λ_{cal}) non radiative relaxation rates (W_{NR}) and quantum efficiencies (η) for ⁴F_{9/2} state of Dy³⁺ doped lithium fluoroborate glasses. From the data, it observed that the experimental life times are lower than the calculated life times in all glass matrices. This is mainly due to the presence of non-radiative channels. Among the prepared glasses, BZL0.3D glass exhibit higher quantum efficiency corresponding to the ⁴F_{9/2} energy level as 68% and is suggested as a potential material for

laser applications.

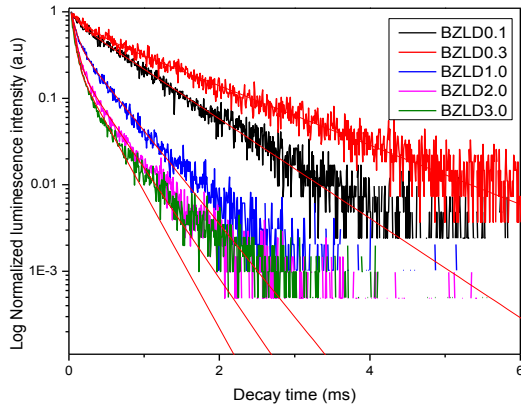


Figure 7. Decay profile corresponding to the $^4F_{9/2}$ energy level of the Dy^{3+} doped lithium fluoroborate glasses

Table 7. The calculated (λ_{cal}) experimental (λ_{exp}) lifetime, quantum efficiency η (%) energy transfer parameter (Q), critical transfer distance (R_0) Energy Transfer rate (C_{DA}) and the non-radiative transition (W_{NR}) of the Dy^{3+} doped lithium fluoroborate glasses

Glass code	λ_{cal}	λ_{exp}	η (%)	W_{NR}
BZL0.1D	9400	730	7.7659	0.001263
BZL0.3D	1729	1180	68.2475	0.000269
BZL1.0D	1198	330	27.5459	0.002196
BZL2.0D	1135	222	19.5594	0.003623
BZL3.0D	1206	179	14.8424	0.004757

White Light Emission

The assessment and quantification of color is referred as colorimetry and the CIE system is the commonly used method to describe the composition of any color. The color of the luminescent source can be described through the color matching function values and they are dimensionless quantities. The degree of stimulation required to match the color of spectral power density $p(\lambda)$ is expressed as,

$$X = \int \bar{x}(\lambda)p(\lambda)d\lambda$$

$$Y = \int \bar{y}(\lambda)p(\lambda)d\lambda$$

$$Z = \int \bar{z}(\lambda)p(\lambda)d\lambda$$

where X, Y, Z are the tristimulus values which gives the power for each of three primary colors to match with the color of $p(\lambda)$ and from the tristimulus values the color chromaticity coordinates x and y can be determined from the following expression,

$$x = \frac{X}{X+Y+Z}$$

$$y = \frac{Y}{X+Y+Z}$$

The (x, y) coordinates are used to represent the color and locus of all the monochromatic color coordinates which produces the perimeter of the CIE1931 chromaticity diagram. All the multi chromatic wavelengths are expected to lie within the area of chromaticity diagram. The luminescent intensity of the emission spectral measurements has been characterized using the CIE1931 chromaticity diagram.

The x, y color chromaticity coordinates of the Dy^{3+} doped lithium fluoroborate glasses have been determined and presented in table 8 along with the x, y color chromaticity coordinates of the reported Dy^{3+} doped systems. The chromaticity coordinates are found to be (0.33, 0.31), (0.32, 0.30), (0.30, 0.31), (0.28, 0.28), and (0.29, 0.28) corresponding to the BZL0.1D, BZL0.3D, BZL1.0D, BZL2.0D and BZL3.0D glasses respectively. Figure 8 represents the location of chromaticity coordinates of Dy^{3+} doped title glasses on CIE1931 chromaticity diagram. The chromaticity coordinates of the title glasses appear in the near white light region of the CIE1931 chromaticity diagram. Though they are in the white light region they emit yellowish white light but there is a tendency to move towards the exact white light region due to the decreasing Y/B ratio values.

The correlated color temperature (CCT) has been calculated using the color coordinates employing the McCamy's approximate formula.

$$CCT = -449n^3 + 352n^2 - 6823n + 5520.33$$

where $n = (x - x_e)/(y - y_e)$ is the inverse slope line $x_e = 0.332$, $y_e = 0.186$ is the epicentre. The CCT values of the prepared glasses are presented in Table 9 and compared with the reported Dy^{3+} doped system [19, 20, 24].

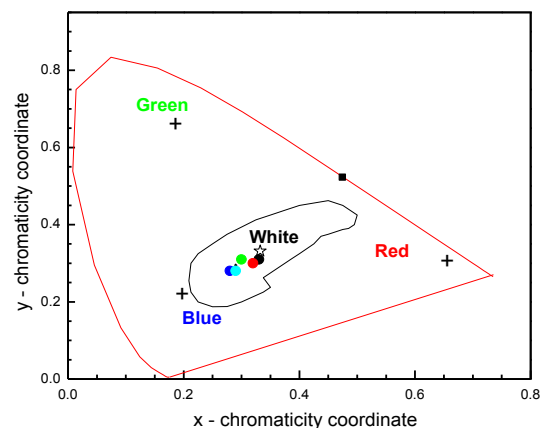


Figure 8. CIE Color Chromaticity diagram of the Dy³⁺ doped lithium fluoroborate glasses

Table 8. Yellow to blue (Y/B) intensity ratio, chromaticity color coordinates (x, y) and correlated color temperature (CCT, K) of the Dy³⁺ doped lithium fluoroborate glasses with the reported Dy³⁺ doped glasses

Glass Code	Y/B ratio	X	Y	CCT	Ref
BZL0.1D	1.2134	0.33	0.31	5531	[Present work]
BZL0.3D	1.207	0.32	0.30	5596	[Present work]
BZL1.0D	1.1987	0.30	0.31	5727	[Present work]
BZL2.0D	1.212	0.28	0.28	6081	[Present work]
BZL3.0D	1.216	0.29	0.28	5935	[Present work]
LFBMDy10	1.047	0.44	0.42	3080	6
LBO:xDy ³⁺	0.949	0.344	0.37	-	11
1.0LBTPD	-	0.26	0.31	-	19
BTLN2D	1.889	0.39	0.45	4034	20
Lithium fluoroborate	0.600	0.29	0.34	7416	24

Conclusion

The Dy³⁺ doped lithium fluoroborate glasses were prepared and their structural and optical properties were studied through XRD, absorption and luminescence spectral measurements. The XRD pattern confirms the amorphous nature of the prepared glasses. Negative δ values indicate the ionic nature of the Dy³⁺-O bond in the prepared glasses. The peak wavelength and effective bandwidth were calculated for ⁴F_{9/2}→⁶H_{15/2} and ⁶H_{13/2} transitions through the luminescence spectra and the results were reported. The x, y coordinates of the prepared glasses are located in the white light region of the CIE diagram and thus suggests their suitability for white light applications.

References

- [1] P.Babu, C.K.Jayasankar, Journal of optical materials 15(2000) 65-79.
- [2] J.S. Kumar, A.M. Bahu, N.K. Giri, S.B. Rai, L.R. Moorthy Journal of Luminescence 130 (2010) 1916-1923.
- [3] R.T Karunakaran, K. Marimuthu, S.SurendraBabu, S.Arumugam, Journal of Luminescence 130(2010) 1067-1072.
- [4] I. Arul Rayappan, K. Marimuthu, Journal of Non-Crystalline Solids 367 (2013) 43-50.
- [5] M.V. Sasikumar, D.Rajesh, A.Balakrishna, Y.C.Ratnakaram Journal of Molecular Structure 1041 (2013) 100-105.
- [6] A. Balakrishna, D. Rajesh, Y.C. Ratnakaram Journal of Luminescence 132 (2012) 2984-2991.
- [7] R.Vijayakumar, K Marimuthu Journal of Molecular Structure 1092 (2015) 166-175.
- [8] Kummara Venkata Krishnaiah, Kagola Upendra Kumar et al. Mater. Express, Vol. 3, No. 1, 2013.
- [9] P.P. Pawar, S.R. Munishwar, R.S. Gedam Journal of Alloys and Compounds 660 (2016) 347e355.
- [10] D.D. Ramteke, R.S. Gedam Spectroscopy letters 48 (2015) 417-421.
- [11] Xin-Yuan Sun, Shuai Wu, Xi Liu, Pan Gao, Shi-Ming Huang Journal of Non-Crystalline Solids 368 (2013) 51-54.
- [12] K. Annapoorani, Ch. Basavapoornima, N. Suriya Murthy, K. Marimuthu Journal of Non-Crystalline Solids 447 (2016) 273-282.
- [13] R.T. Karunakaran, k.Marimuthu, S.SurendraBabu, Physica B 404 (2009) 3995-4000.
- [14] G.S. Ofelt Journal of Chem. Phys.37 (1962) 511.
- [15] A Renuka Devi, C.K. Jayasankar, Non-Crystalline Solids 197 (1997) 111.
- [16] O. Ravi C. Madhukar Reddy, B. Sudhakar Reddy, B. Deva Prasad Raju Optics Communications, (2014) 312:263.
- [17] S.A. Saleem, B.C.Jamalaiah, M. Jayasimhadri et al. Journal of Quantitative Spectroscopy & Radiative Transfer 112 (2011) 78-84.
- [18] B.C. Jamalaiah, L. RamaMoorthy, Hyojinseo, Journal of Non Crystalline Solids 358 (2012) 204-209.
- [19] S. Selvi, G Venkataiah, S. Arun Kumar, G. Muralidharan, K. Marimuthu Physics B 454 (2014) 72-81.
- [20] V. Uma, K. Maheshvaran, K. Marimuthu, G.Muralidharan. Journal of Luminescence 176 (2016) 15-24.
- [21] L Vijayalakshmi, V. Naresh B.H. Rudramadevi, S. Buddhudu International Journal of Engineering and Science Vol.4, Issue 9 (2014) 19-25.
- [22] R.T. Karunakaran, K. Marimuthu, S. Surendra Babu, S. Arumugam Physics B 404(2009) 3995-4000.
- [23] S.A. Azizan, S Hashim, N.A. Razak, M.H.A. Mhareb Journal of Molecular Structure 176 (2014) 20-25.
- [24] Sd.Z.A. Ahamed, C.M. Reddy, B.D.P. Raju, Opt. Mater. 35 (2013) 1385-1394.